Am J Transl Res 2020;12(5):1839-1850
www.ajtr.org /ISSN:1943-8141/AJTR0106648

Original Article

Glioma-associated oncogene homolog 1 stimulates FOXP3 to promote non-small cell lung cancer stemness

Haolong Qi[1,2*], Wende Li[3*], Jie Zhang[4*], Jianxin Chen[5], Jia Peng[2], Yi Liu[2,6], Shucai Yang[7], Jing Du[8], Xiang Long[8], Calvin SH Ng[2], Ming-Yue Li[2,9,10], George G Chen[2,6,9]

[1]Department of Hepatobiliary Surgery, Renmin Hospital of Wuhan University, Wuhan, Hubei, China; [2]Department of Surgery, The Chinese University of Hong Kong, Prince of Wales Hospital, Shatin, NT, Hong Kong, China; [3]Guangdong Key Laboratory of Laboratory Animal, Guangdong Laboratory Animals Monitoring Institute, Guangzhou, Guangdong, China; [4]Department of Thyroid and Breast Surgery, Zhongnan Hospital of Wuhan University, Wuhan, Hubei, China; [5]Department of Surgery, Jiangxia District Hospital of Traditional Chinese Medicine, Wuhan, Hubei, China; [6]Guangdong Key Laboratory for Research and Development of Natural Drugs, Guangdong Medical University, Zhanjiang, Guangdong, China; [7]Department of Clinical Laboratory, Pingshan District People's Hospital of Shenzhen, Shenzhen, Guangdong, China; [8]Peking University Shenzhen Hospital, Shenzhen, Guangdong, China; [9]Shenzhen Research Institute, The Chinese University of Hong Kong, Shenzhen, Guangdong, China; [10]Guangzhou Regenerative Medicine and Health Guangdong Laboratory, Guangzhou, Guangdong, China. [*]Equal contributors.

Received December 19, 2019; Accepted April 20, 2020; Epub May 15, 2020; Published May 30, 2020

Abstract: Glioma-associated oncogene homolog 1 (GLI1), an oncogenic molecule in non-small cell lung cancer (NSCLC), promotes the growth of NSCLC by enhancing lung cancer stem cells (LCSCs). However, the mechanism responsible remains unknown. FOXP3 is known to maintain LCSCs. The aim of this study was to explore whether GLI1 enhanced LCSCs via stimulating FOXP3. Experiments were performed in NSCLC tissue samples, cell lines and the animal tumor model. The expression of GLI1- and LCSC-related molecules was assessed at protein and mRNA levels. Relevant cell functions were also determined. A tumor xenograft mouse model was established to confirm the oncogenic role of GLI1. We confirmed that the expression of GLI1 was up-regulated in the tumor tissues of NSCLC compared with adjacent non-tumor tissues. But no significant association between GLI1 and clinicopathological characteristics was found. GLI1 expression was positively correlated with FOXP3 and it could promote FOXP3 expression likely via acting on the promoter of FOXP3. Along with the upregulation of FOXP3, GLI1 increased the expression of LCSC markers, ALDH1A1 and OCT4A, and the formation of tumor spheres, whereas the inhibition of GLI1 decreased the above features. We also found the involvement of Notch1 activation in GLI1-mediated FOXP3 pathway. The *In vivo* mouse tumor model verified the positive role of GLI1 in the growth of the tumor. Collectively, this study has demonstrated that GLI1 stimulates FOXP3 to promote LCSCs.

Keywords: Glioma-associated oncogene homolog 1, FOXP3, lung cancer, cancer stem cells, Notch1

Introduction

Glioma-associated oncogene homolog 1 (GLI1), initially identified as an amplified gene in a human malignant glioma, is a member of the Kruppel family of zinc finger-containing transcription factors. As a key molecule in Hedgehog signaling pathway, GLI1 plays a positive role in the development/growth of several types of human cancers including non-small cell lung cancer (NSCLC) [1, 2]. The positive role of GLI1 in NSCLC has been demonstrated by clinical observations and inhibitory experiments [3-10]. GLI1 expression is associated with poor survival, unfavorable clinical outcome and metastasis [5, 7], and contributes to the resistance to anti-tumor treatments [3, 10]. The inhibition of GLI1 can significantly arrest the growth of NSCLC and sensitize cancer cells to anti-tumor treatments [6, 8, 9].

A number of publications have further revealed that the inhibition of GLI1 contributes to the suppression of lung cancer stem cells (LCSCs)

[11-17], a small subset of lung cancer cells that are critical for tumor growth, metastasis, recurrence and resistance to treatments [18]. A number of endogenous molecules or synthetic agents including Raf kinase inhibitory protein, arsenic trioxide, GANT61, sodium selenite, and triptonide have been demonstrated to downregulate LCSCs via inhibiting GLI1 [13-17]. These data have strongly suggested that the inhibition of GLI1 can be an alternative therapeutic strategy to improve the treatment for NSCLC. However, how GLI1 is associated with LCSCs remains largely unknown.

Forkhead box P3 (FOXP3), a classic marker for regulatory T cells, is now known to express in cancer cells [19]. Our early study has shown that the expression of FOXP3 is highly increased in NSCLC, and it can stimulate the Wnt-β-catenin signaling pathway to induce epithelial-mesenchymal transition (EMT) [20]. EMT is known to upregulate LCSCs by increasing the expression of molecules related to LCSCs [2, 20, 21]. In fact, the expression of FOXP3 has been reported to be associated with maintenance/survival of stem cells [22-24]. We therefore hypothesized that GLI1 inhibition-mediated downregulation of LCSCs was via the negative regulation of FOXP3 in NSCLC. Both *in vitro* and *in vivo* experiments were performed to explore how GLI1 regulated FOXP3 expression in NSCLCs, and to determine the impact of GLI1 and FOXP3 interaction on lung cancer cell stemness.

Materials and methods

Ethics statement

All experiments on human subjects followed the Helsinki Declaration (as revised in 2013). The human tissue specimens were collected after the written informed consent was obtained. The use of human samples in this study was approved by the joint Chinese University of Hong Kong (CUHK)-New Territories East Cluster Clinical Research Ethics Committee. All animal experiments were approved by the Animal Experimentation Ethics Committee of CUHK.

Database analysis

The UCSC Xena platform (http://xena.ucsc.edu/) for public and private cancer genomics data visualization and interpretation was used in this research. This database is based on TCGA (The Cancer Genome Atlas) to provide an access to integrated TCGA data sets according to the types of tissue samples. Four sets of NSCLC data were included in this analysis: 2 sets for lung adenocarcinoma and 2 sets for lung squamous cell carcinomas. The expression of GLI1 and FOXP3 detected by RNA sequencing was extracted, and then the linear regression was used to construct the correlation between the two genes. When the *P* value was below 0.05, the correlation was deemed to be significant.

Tissue collection

87 pairs of NSCLC tissues and the corresponding adjacent non-tumor lung tissues were obtained from patients who were surgically treated in Prince of Wales Hospital from 2003 to 2016. All the patients were diagnosed with NSCLC through laboratory tests and imaging examinations before surgery, and histopathological evaluations were done after surgery. The summary of clinical characteristics was shown in **Table 1**. No patients received any local or systemic treatment before surgery. A portion of the collected tissue samples was fixed in formalin for histological evaluation, and the other portion of the samples was snap-frozen in liquid nitrogen and stored at -80°C until experiments. Chi-square analysis was used to evaluate the correlation of the clinical characteristics with the expression of GLI1.

Immunohistochemistry assay

Immunohistochemistry assay (IHC) was performed on formalin-fixed paraffin sections according to the standard protocol using primary antibodies to GLI1 (Novus Biologicals, 1:500) and FOXP3 (Santa Cruz, 1:50). The staining intensities were scored using the immunoreactive score (IRS) method by a pathologist and an investigator separately. The IRS method was shown in **Table 2**.

Cell lines and culture conditions

NSCLC cell lines NCH-H460 and NCH-H23 were obtained from the American Type Culture Collection (ATCC), and cultured in RPMI 1640 (Invitrogen, Carlsbad, CA) with 10% fetal bovine serum and antibiotics at 37°C in humidified air with 5% CO_2 or with 1% O_2.

Table 1. Clinical characteristics of the patients

	Total	GLI1		
		H	L	
Smoking Status				P>0.05
Smoker	60	49	11	
Nonsmoker	27	26	1	
Gender				
Male	59	48	11	P>0.05
Female	28	27	1	
Age (Y)	66.16±7.92	66.43±0.94	64.50±1.78	P>0.05
Tumor Differentiation				P>0.05
Adenocarcinomar	45	41	4	
Squarmas Carcinomar	20	16	4	
Poor Differentiation	22	18	4	
Stage				P>0.05
IA	26	23	3	
IB	18	16	2	
IIA	13	11	2	
IIB	14	10	4	
IIIA	11	11	0	
IIIB	2	1	1	
IV	3	3	0	
T Stage				P>0.05
1	33	30	3	
2	38	33	5	
3	14	11	3	
4	2	1	1	
Lymph Metastasis				P>0.05
Positive	26	22	4	
Negative	61	53	8	

H: high expression; L: low expression.

Table 2. Expression and scoring of GLI1 in patient NSCLC tissues

Intensity / Positive Cell (%)	Weak Staining = 1 point	Medium Staining = 2 points	Strong Staining = 3 points
<10% = 1 point	IRS = 1	IRS = 2	IRS = 3
10%-<50% = 2 points	IRS = 2	IRS = 4	IRS = 6
50%-<80% = 3 points	IRS = 3	IRS = 6	IRS = 9
≥80% = 4 points	IRS = 4	IRS = 8	IRS = 12

Transfection of cell lines and construction of stably transfected cell lines

hGli1-6x-his (a plasmid based on pcDNA3.1) was a gift from Martin Fernandez-Zapico (Addgene plasmid #84923; http://n2t.net/addgene: 84923; RRID: Addgene_84923). The empty of pcDNA3.1 vector was used as a control for GLI1 expression. The plasmid of pLKO.1 was used as backbone for the construction of shRNAs, and it was also used as a control for shRNAs. The shRNAs for GLI1 were constructed according to the protocol of Genetic Perturbation Platform (www.broadinstitute.org), and the sequence used was shown in **Table 3**. The overexpression plasmids of pHIV-FOXP3 and shRNAs for FOXP3 were constructed as described before [20]. The pHIV empty vector was used as a control for pHIV-FOXP3. After transfection or lentivirus infection, the cells were screened by G418 or puromycin for different durations according to the respective instructions of the suppliers.

Western blot analysis

A lysis buffer containing the mammalian protein extraction reagent RIPA (Beyotime, China), a protease inhibitor cocktail (Roche, Basel, Switzerland) and PMSF (Roche, Basel, Switzerland) were used to lyse the cells after treatments. The protein concentration was determined by the Bradford method using Bradford DC. Samples containing 20 μg of protein from each cell line were electrophoresed. The protein was transferred onto 0.22 μm nitrocellulose membranes (Millipore, Bedford, MA). After the protein was blocked in 5% skim milk for 1 h at room temperature, the membrane was incubated with a relevant primary antibody at 4°C overnight. After incubation with the corresponding secondary antibody conjugated to horseradish peroxidase, the enhanced chemiluminescence chromogen-

Table 3. Primers used for shRNA construction

shRNA	Forward	Reverse	Target Seq
shGLI1	5'-CCGGCATCCATCACAGATCGCATTTCTC-GAGAAATGCGATCTGTGATGGATGTTTTTG-3'	5'-AATTCAAAAACATCCATCACAGATCG-CATTTCTCGAGAAATGCGATCTGTGATGGATG-3'	5'-CATCCATCACAGATCG-CATTT-3'

ic substrate (Griffin Biotech, Hong Kong, China) and photo plates (Kodak, Rochester, NY) were used to detect specific bands on the membrane. Antibodies for GLI1 (Novus Biologicals, CO), FOXP3 (Cell Signaling, Danvers, MA), OCT4A (Cell Signaling, Danvers, MA), ALDH1A1 (Santa Cruz, CA), Notch1 (Cell Signaling, Danvers, MA) and HES1 (Cell Signaling, Danvers, MA) were used as primary antibodies. Protein expression was semi-quantified by the control β-tubulin (Santa Cruz, CA) or GAPDH (Santa Cruz, CA) (Supplemental Figure 1). The grey scale ratio was assessed by Adobe Photoshop CS6 (San Jose, CA). The photos were the representative from the triple experiments.

Cell proliferation assays

The MTT kit (Sigma, St. Louis, MO) was used to assay the cell proliferation and conducted according to the manufacturer's instruction. Transfected and negative control H460 cells or H23 cells were harvested 24 h after transfection, and then, they were cultured on 96-well plates for different periods. 10 μl of MTT was added to each well, and the OD490 was assessed after 4 h.

Cell invasion assay

At 24 h after transfection, approximately 5 × 10^5 transiently transfected or negative control cells in serum-free media were cultured in the upper chamber for migration assays (8 μm pore size, Millipore, Burlington, MA) and invasion assays with 20% Matrigel (Sigma, St. Louis, MO). The lower chambers were filled with 600 μl of RPMI 1640 media containing 20% FBS. After 24 h of incubation at 37°C, the cells that had migrated or invaded through the membrane were fixed in 4% paraformaldehyde and stained with 0.1% crystal violet (Sigma, St. Louis, MO). The cells below the surface were photographed, and the cells in three random fields were counted.

Colony formation

After 3000 stably transfected cells were cultured in each well of a 6-well plate for 10 to 14 days, colonies containing more than 50 cells were counted.

Tumor sphere formation

5000 stably transfected cells were cultured in each well of a 6-well ultra-low attachment plate (Corning) for 10 days. All the cells were cultured in Cancer Stem Premium (ProMab, CA) at 37°C in humidified air with 5% CO_2. The tumor spheres containing more than 50 cells were counted. Tumor sphere forming efficiency was calculated by dividing the number of tumor spheres formed (≥50 μM) by the original number of single cells seeded and was expressed as the mean percentage of the efficiency.

Dual-luciferase reporter assay

H460 and H23 cells were plated in 12-well plates and co-transfected with various plasmids as indicated in the figures. Cells were collected 48 h after transfection, and luciferase activities were analyzed by the dual-luciferase reporter assay kit (Promega, Fitchburg, WI). Reporter activity was normalized to the control Renilla. hGli1-6x-his was a gift from Martin Fernandez-Zapico (Addgene plasmid #84923; http://n2t.net/addgene: 84923; RRID: Addgene_84923), and it was used as GLI1 DNA here. The plasmid of pcDNA3.1 was used as a control for GLI1 DNA.

Tumor xenograft assay

Female nude mice, 6-8 weeks old, were provided by Laboratory Animal Service Center of CUHK, and kept on a 12-h light, 12-h dark cycle with free access to food and water. 2 × 10^6 H460-GLI1 and H460-Control cells were subcutaneously inoculated respectively into the left and right flank in the back of the nude mice for tumor xenograft experiments. Tumor size was measured every 3 days for 15 days by a micrometer. Tumor volume was calculated by length × width × width/2. Tumors were harvested and fixed in formalin for histological evaluation or snap frozen in liquid nitrogen for both mRNA and protein preparations.

Statistical analysis

In this study, when the gene expression in the tumor tissue was equal or higher than in the corresponding normal tissue, the corresponding patient tissue would be defined as a high expression sample, whereas when the gene expression in the tumor tissue was lower than in the corresponding normal tissue, the patient tissue would be considered as a low expression sample. Paired t-test was used to evaluate the expression levels of GLI1 and FOXP3 in NSCLC tissues. Other data were analyzed by Student t-test. Statistical analysis was done suing GraphPad Prim 6.0 software (GraphPad, La Jolla, CA). *P*-values of less than 0.05 were considered statistically significant.

Results

The expression of GLI1 and its association with clinical characteristics

The expression of GLI1 in patient tissues was evaluated by IHC. It showed that the expression of GLI1 was upregulated in tumor tissues compared with adjacent normal tissues (**Figure 1A** and **1B**). However, there was not any significant association between GLI1 levels and clinicopathological features (**Table 1**).

The influence of GLI1 on FOXP3 expression on cancer cells

As our previous report, the expression of FOXP3 was upregulated in tumor tissues compared with the adjacent normal tissues [18], and the finding was confirmed in this study (**Figure 1C** and **1D**). Furthermore, the linear regression analysis showed that there was a significantly positive correlation between the expression of GLI1 and FOXP3 (**Figure 1E** and **1F**).

The oncogenic role of GLI1 was evident in NSCLC cells with the GLI1 overexpression

The levels of FOXP3 and two CSC markers, ALDH1A1 and OCT4A were upregulated in the GLII-overexpressed cells (**Figure 2A**). As shown by the luciferase reporter assay, GLI1 could promote the activity of FOXP3 promotor (**Figure 2B**). Cells with the GLI1 overexpression were more proliferative and invasive than the controls as demonstrated by MTT assay, transwell assay and colony formation assay respectively (**Figures 3A**, **4A** and **4C**). In contrast, the knockdown of GLI1 by its shRNA inhibited the expression of FOXP3 (**Figure 2A**), the cell proliferation (**Figure 3B**), invasion (**Figure 4B**), and colony formation (**Figure 4D**). H460 cells with stable expression of GLI1 were subcutaneously injected into nude mice to conduct xenograft experiments. The results indicated that GLI1 could significantly promote the growth of NSCLC tumors (**Figure 3C**).

According to the results of database analysis, among lung adenocarcinomas, there was a positive correlation in the RNA expression between GLI1 and FOXP3 (**Figure 5A** and **5C**), which was in line with the result of our own NSCLC analysis (**Figure 1**). However, there was no relationship between the two molecules in lung squamous cell carcinomas (**Figure 5B** and **5D**).

The influence of FOXP3 on cancer stemness markers and Notch pathway

When the expression of FOXP3 was upregulated in NSCLC cells, the levels of LCSC markers ALDH1A1 and OCT4A were increased (**Figure 2C**), suggesting a positive effects of FOXP3 on cancer stemness. The overexpression of FOXP3 also increased the levels of Notch1 and HES1, indicating that the Notch pathway was activated by FOXP3.

The upregulation of cancer stemness by GLI1

As indicated above, GLI1 overexpression could significantly enhance the expression of two LCSC markers, ALDH1A1 and OCT4A (**Figure 2A**). More importantly, GLI1 markedly promoted the formation of tumor spheres in H23 and H460 cells (**Figure 4E**). Therefore, GLI1 overexpression could enhance the stemness of NSCLC cells. The positive role of GLII on LCSCs was confirmed by the inhibitory analysis. The knockdown of GLI1 by its shRNA obviously reduced the expression of ALDH1A1 and OCT4A (**Figure 2A**), and the formation of tumor spheres (**Figure 4F**).

Discussion

In this study, we confirmed GLI1 as an oncogenic molecule in NSCLC by the following tests. First, the expression of GLI1 was significantly higher in the tumor tissues of NSCLC than the

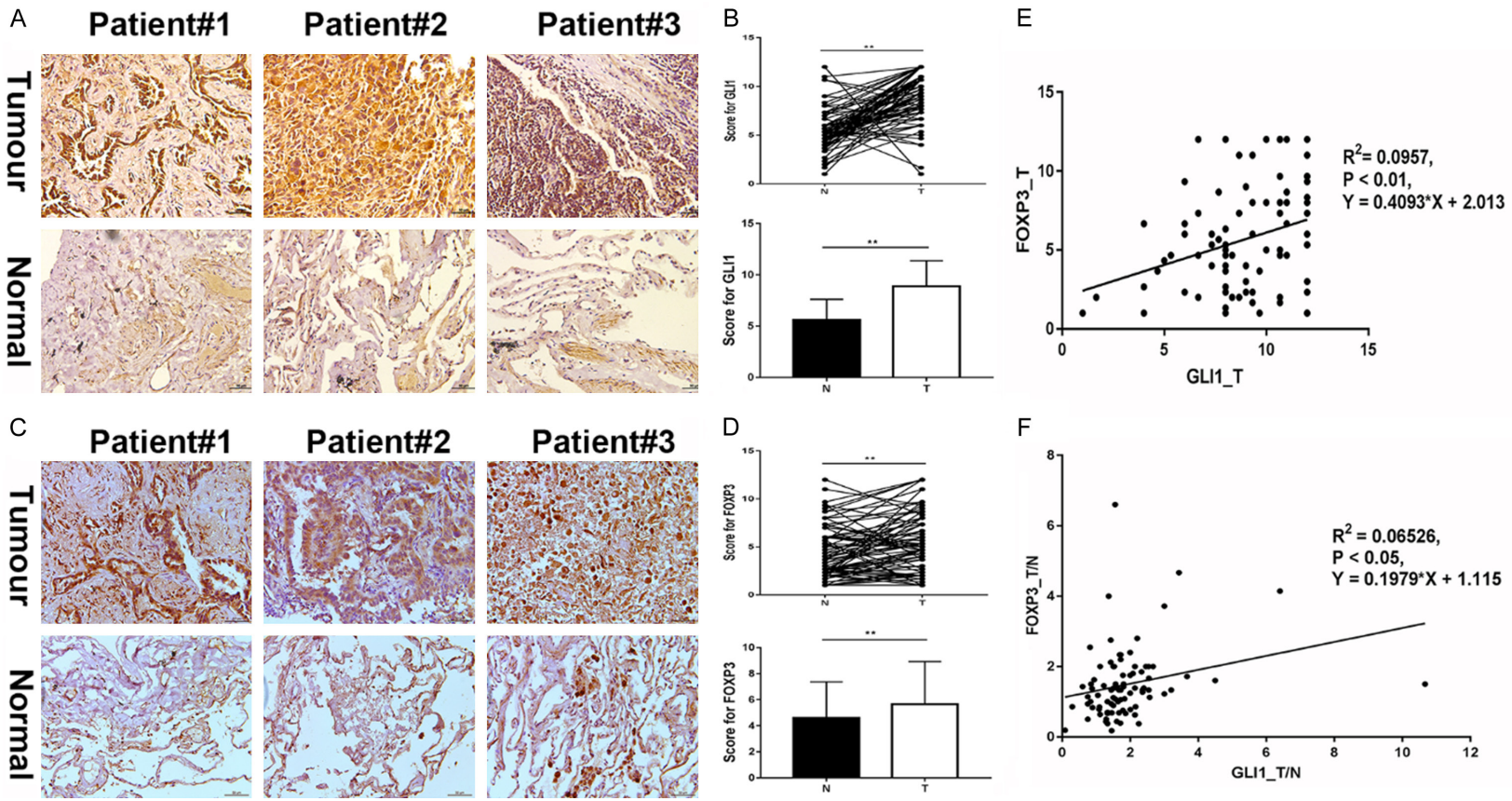

Figure 1. The expression of GLI1 and FOXP3 in NSCLC. A. The representative IHC results of GLI1 expression in patient tissues. B. The expression of GLI1 was up-regulated in tumor tissues (T) compared with adjacent normal tissues (N), **P<0.01. C. The representative IHC results of FOXP3 expression in patient tissues. D. The expression of FOXP3 was upregulated in tumor tissues (T) compared with adjacent normal tissues (N), **P<0.01. E. The correlation of the relative IHC scores between GLI1 and FOXP3 in tumor tissues (T). F. The correlation of the relative IHC scores between GLI1 and FOXP3. T/N: Values that derived from scores of tumor tissues divided by the corresponding scores of adjacent normal tissues. Data were analyzed by paired t-test. Linear regression was used to construct the correlation between the two genes. When the *P* value was below 0.05, the correlation was deemed to be significant.

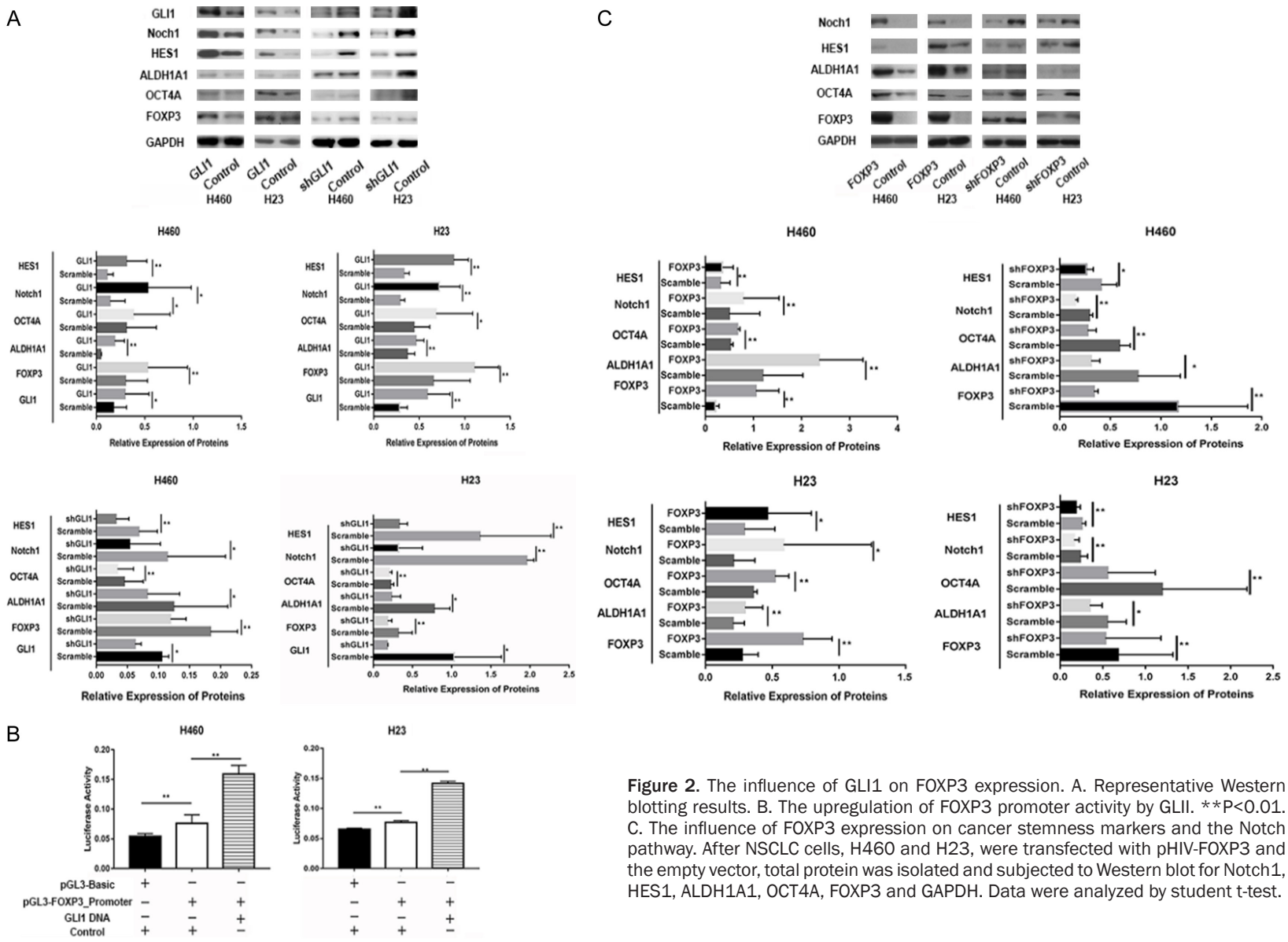

Figure 2. The influence of GLI1 on FOXP3 expression. A. Representative Western blotting results. B. The upregulation of FOXP3 promoter activity by GLII. **P<0.01. C. The influence of FOXP3 expression on cancer stemness markers and the Notch pathway. After NSCLC cells, H460 and H23, were transfected with pHIV-FOXP3 and the empty vector, total protein was isolated and subjected to Western blot for Notch1, HES1, ALDH1A1, OCT4A, FOXP3 and GAPDH. Data were analyzed by student t-test.

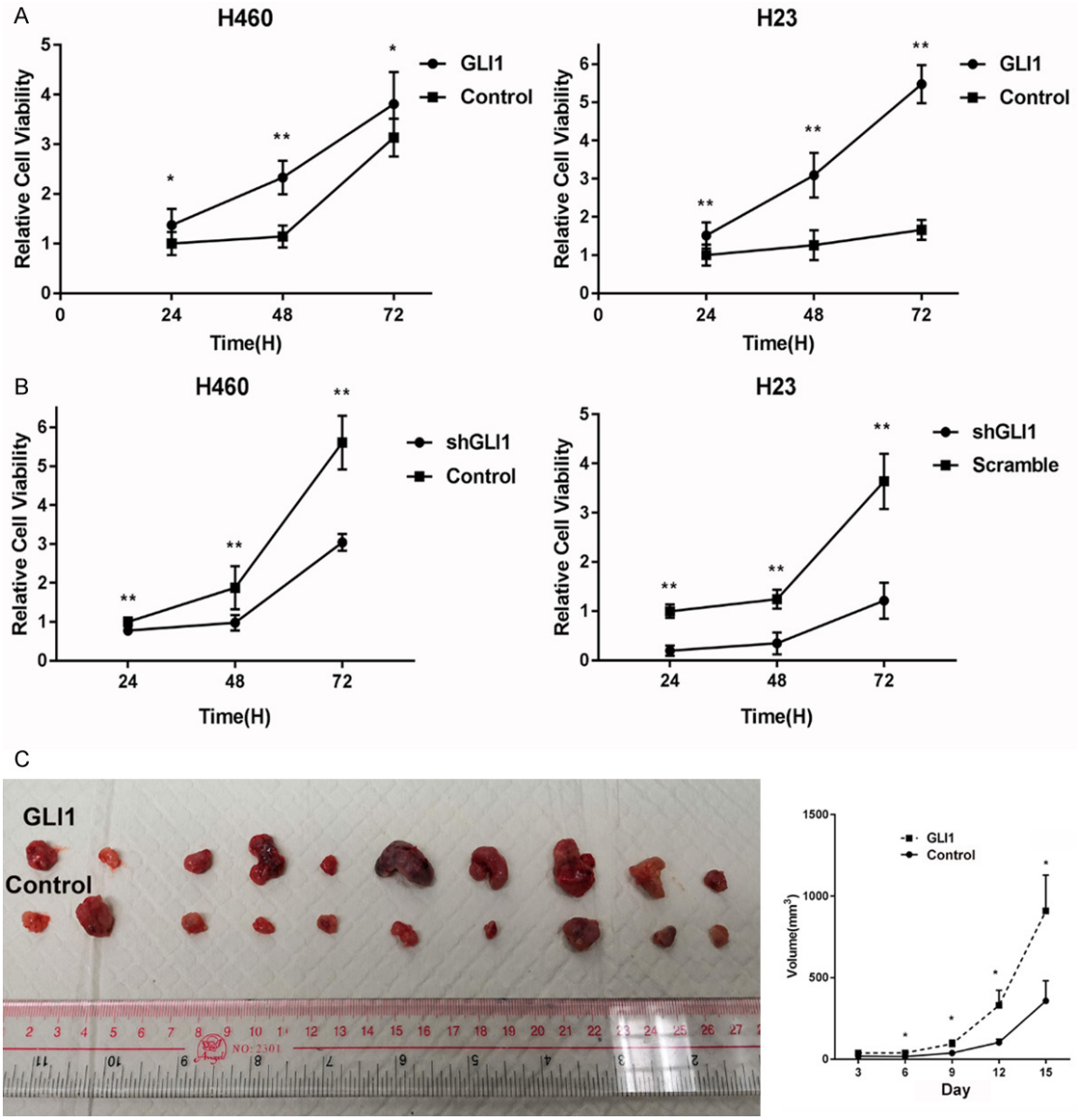

Figure 3. GLI1 promotes NSCLC cell proliferation and growth *in vitro* and *in vivo*. A. After NSCLC H460 and H23 cells were transfected with GLI1 DNA and the empty vector, MTT assay was performed to measure cell proliferation. *P<0.05, **P<0.01. B. After NSCLC H460 and H23 cells were treated with GLI1 shRNA, MTT assay was performed to measure cell proliferation. **P<0.01. C. Nude mice were subcutaneously implanted with GLI1-overexpressed H460 cells. The growth of the tumor was monitored every 3 days for 15 days. At the end of the study, the tumor was collected and the size of tumor was measured. *P<0.05. Data were analyzed by student t-test.

matched non-tumor tissues. Second, the overexpression of GLI1 promoted the oncogenic functions of NSCLC cells including cell proliferation, invasion and colonic formation, whereas the inhibition of GLI1 diminished these the oncogenic functions. Third, GLI1 was able to stimulate the expression of LCSC biomarkers including ALDH1A1 and OCT4A [2, 18], and to increase the formation of tumor spheres. And finally, the tumor formed by NSCLC cells with GLI1 overexpression grew much larger than the cells without GLI1 overexpression *in vivo*.

Our study has for the first time demonstrated that the overexpression of GLI1 enhanced the expression of FOXP3 in NSCLC cells, and furthermore, the GLI1-mediated upregulation of FOXP3 was likely through a positive effect of

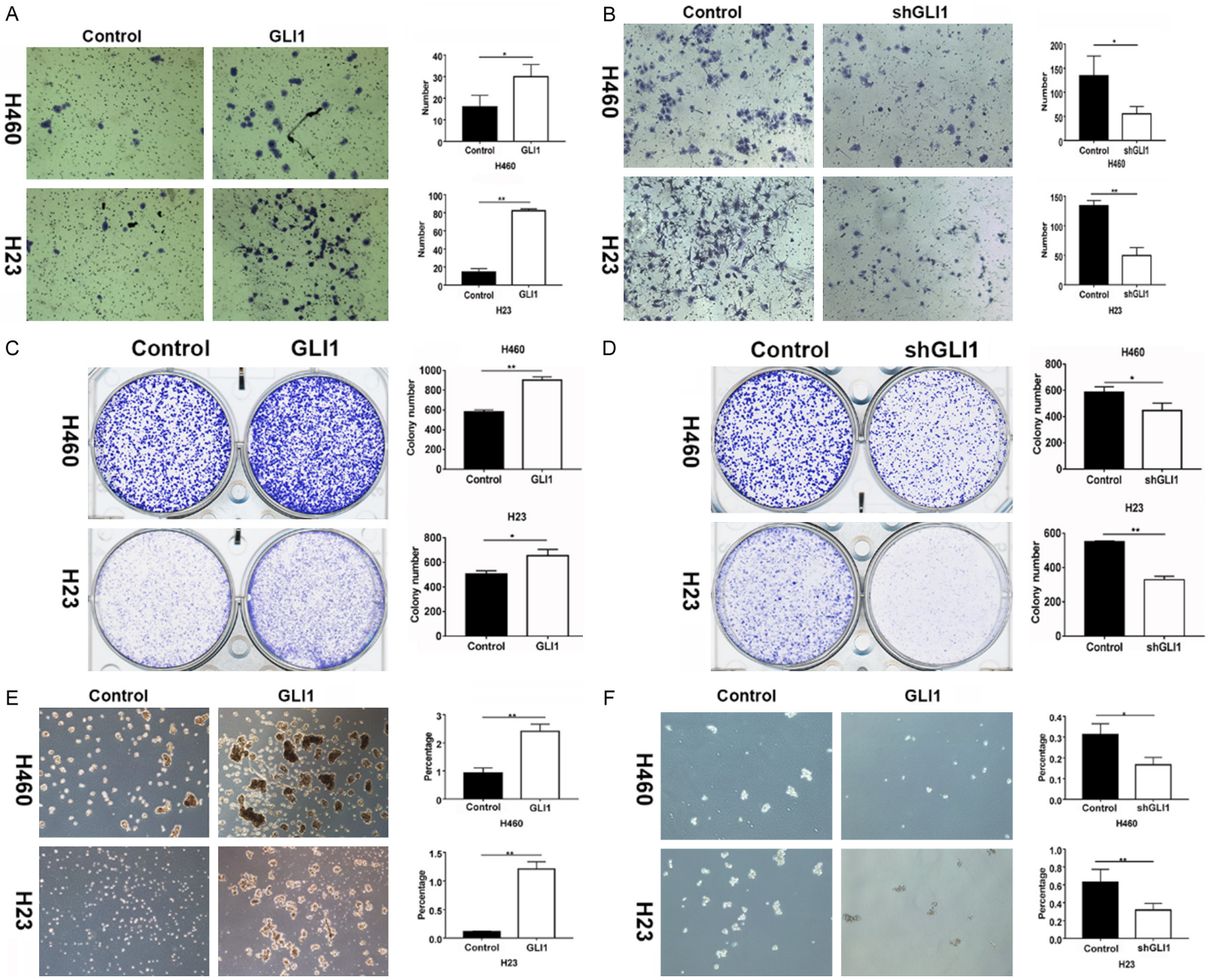
A
Control
GLI1
H460
H23
Number
Control
GLI1
H460
H23
B
Control
shGLI1
H460
H23
Number
Control
shGLI1
H460
H23
C
Control
GLI1
H460
H23
Colony number
Control
GLI1
H460
H23
D
Control
shGLI1
H460
H23
Colony number
Control
shGLI1
H460
H23
E
Control
GLI1
H460
H23
Percentage
Control
GLI1
H460
H23
F
Control
GLI1
H460
H23
Percentage
Control
shGLI1
H460
H23

Figure 4. GLI1 promotes NSCLC cell invasion, anchorage-independent growth ability and cancer stemness. A. Transwell assays for cells with GLI1 overexpression. *P<0.05, **P<0.01. B. Transwell assays for cells with GLI1 knockdown. *P<0.05, **P<0.01. C. The number of colony formation by GLI1-overexpressed cells was counted. *P<0.05, **P<0.01. D. The number of colony formation by GLI1 shRNA-treated cells was counted. *P<0.05, **P<0.01. E. Cancer stem cell sphere formation assay was performed to test GLI1-overexpressed cells. **P<0.01. F. Cancer stem cell sphere formation assays for cells with GLI1 knockdown. *P<0.05, **P<0.01. Data were analyzed by student t-test.

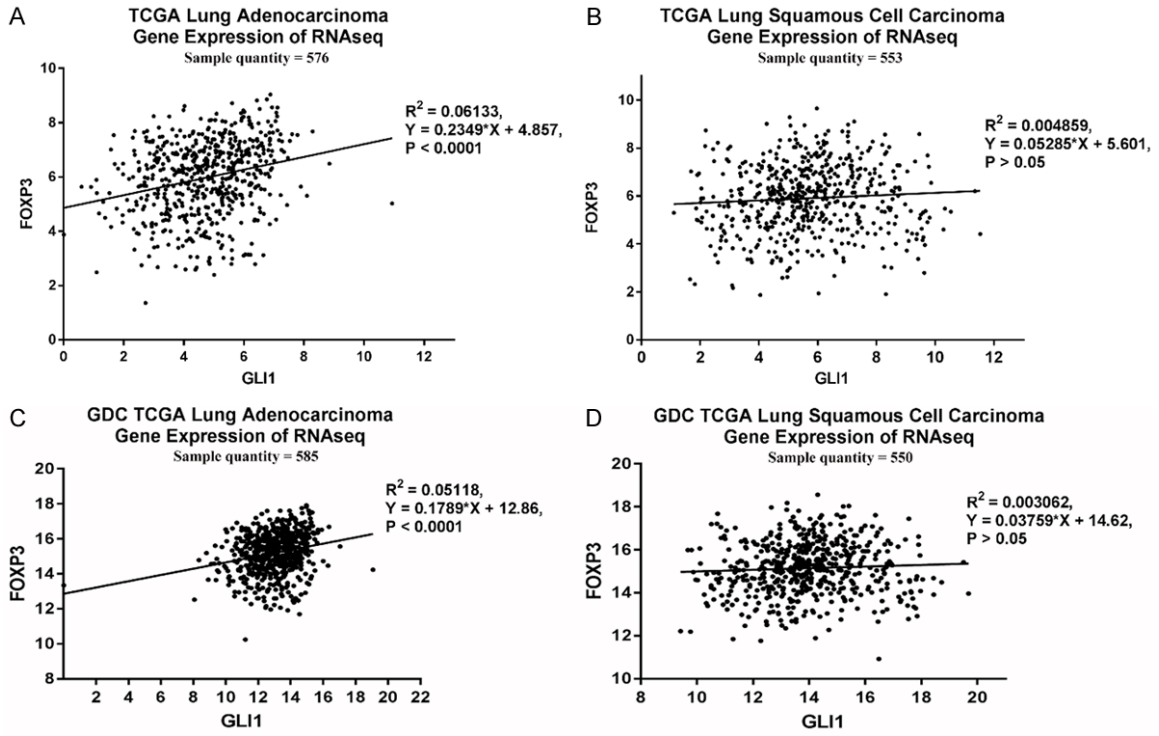

Figure 5. The correlation between GLI1 mRNA and FOXP3 mRNA. A. 576 lung adenocarcinoma samples were included in this data set. B. 553 lung squamous cell carcinoma samples were included in this data set. C. 585 lung adenocarcinoma samples were included in this data set. D. 550 lung squamous cell carcinoma samples were included in this data set. Linear regression was used to construct the correlation between the two genes. When the *P* value was below 0.05, the correlation was deemed to be significant.

GLI1 on the FOXP3 promoter as GLI1 could significantly increase the FOXP3 promoter activity. Along with the GLI1-mediated upregulation of FOXP3, the expression of LCSC biomarkers including ALDH1A1 and OCT4A, and the formation of tumor spheres were increased. These results were verified by the inhibitory experiments as the inhibition of GLI1 by its shRNA downregulated FOXP3, ALDH1A1 and OCT4A, and decreased the formation of tumor spheres. Therefore, the above data have indicated that GLI1 may promote FOXP3 to upregulate LCSCs. This novel mechanism identified is supported by the fact that FOXP3 is a known regulator for stem cells and that FOXP3 can promote the growth of NSCLC by inducing EMT [20, 22-24], an oncogenic feature linked to the induction and maintenance of LCSCs [2, 20, 21]. The connection between GLI1-mediated FOXP3 and LCSCs is in agreement with early studies showing the upregulation of EMT by GLI1 in NSCLC [25, 26].

Our experiment also showed that GLI1-mediated FOXP3 could increase the expression of Notch1 and its downstream target HES1, suggesting the activation of the Notch1 pathway by GLI1-mediated FOXP3. This finding is also supported by the observations that Notch1 can protect the LCSCs from antitumor agent-induced cell death in NSCLC whereas the inhibition of Notch1 facilitates the death of LCSCs [27, 28]. Nevertheless, the detailed Notch1 pathway induced by GLI1-FOXP3 needs further investigation in LCSCs.

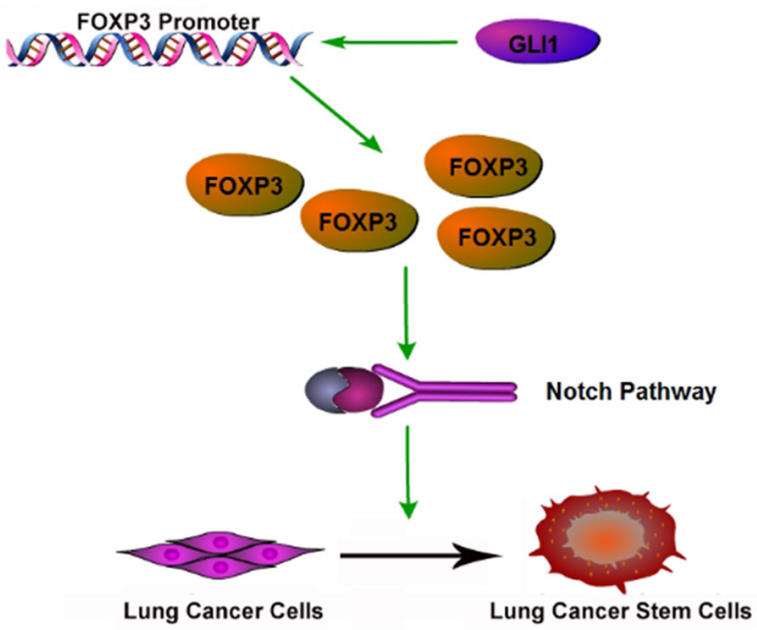

Figure 6. Proposed GLI1-mediated induction of the FOXP3 pathway in the upregulation of LCSCs. GLI1 promotes the expression of FOXP3, and then FOXP3 activates the Notch pathway, resulting in the increase of lung cancer stemness.

In conclusion, we have confirmed the oncogenic role of GLI1 in NSCLC. The expression of GLI1 is positively correlated with the level of FOXP3. Importantly the expression of FOXP3 can be positively regulated by GLI1 likely via stimulating the FOXP3 promoter. The GLI1-mediated FOXP3 can lead to the enhancement of NSCLC cancer stemness, which is associated with the induction of Notch1 (**Figure 6**). We believe that the novel mechanism identified in this study will not only help us to understand how GLI1 induces LCSCs but also provides the new opportunity to improve current NSCLC treatments by interfering with the GLI1-FOXP3 pathway.

Acknowledgements

We thank technical assistance from Ms. Angel Kong. This study was supported by grants from the National Natural Science Foundation of China (No: 81472742). Research Grants Council of the Hong Kong SAR (CUHK462613), Guangdong-Hong Kong Co-operation Project, Guangdong Province (2017A050506031), and the Science and Technology Projects of Guangdong Province (2018B030317001).

Disclosure of conflict of interest

None.

Address correspondence to: George Gong Chen and Mingyue Li, Department of Surgery, Prince of Wales Hospital, Shatin, Hong Kong, China. Tel: +86-852-3505-1541; E-mail: gchen@cuhk.edu.hk (GGC); brightmoonli@yahoo.com (MYL)

References

[1] Mastrangelo E and Milani M. Role and inhibition of GLI1 protein in cancer. Lung Cancer 2018; 9: 35-43.

[2] Aberger F and Ruiz I Altaba A. Context-dependent signal integration by the GLI code: the oncogenic load, pathways, modifiers and implications for cancer therapy. Semin Cell Dev Biol 2014; 33: 93-104.

[3] Cui Y, Cui CA, Yang ZT, Ni WD, Jin Y and Xuan YH. Gli1 expression in cancer stem-like cells predicts poor prognosis in patients with lung squamous cell carcinoma. Exp Mol Pathol 2017; 102: 347-53.

[4] Panneerselvam J, Srivastava A, Mehta M, Chen A, Zhao YD, Munshi A and Ramesh R. IL-24 inhibits lung cancer growth by suppressing GLI1 and inducing DNA damage. Cancers (Basel) 2019; 11.

[5] Jin SD, He J, Li J, Guo RH, Shu YQ and Liu P. MiR-873 inhibition enhances gefitinib resistance in non-small cell lung cancer cells by targeting glioma-associated oncogene homolog 1. Thorac Cancer 2018; 9: 1262-70.

[6] Du J, Chen WW, Yang LJ, Dai JJ, Guo JW, Wu Y, Gong KK, Zhang J, Yu N, Xie Z and Xi SC. Disruption of SHH signaling cascade by SBE attenuates lung cancer progression and sensitizes DDP treatment. Sci Rep 2017; 7: 1899.

[7] Chen W, An J, Guo J, Wu Y, Yang L, Dai J, Gong K, Miao S, Xi S and Du J. Sodium selenite attenuates lung adenocarcinoma progression by repressing SOX2-mediated stemness. Cancer Chemother Pharmacol 2018; 81: 885-95.

[8] Po A, Silvano M, Miele E, Capalbo C, Eramo A, Salvati V, Todaro M, Besharat ZM, Catanzaro G, Cucchi D, Coni S, Di Marcotullio L, Canettieri G,

Vacca A, Stassi G, De Smaele E, Tartaglia M, Screpanti I, De Maria R and Ferretti E. Noncanonical GLI1 signaling promotes stemness features and in vivo growth in lung adenocarcinoma. Oncogene 2017; 36: 4641-52.

[9] Chang KJ, Yang MH, Zheng JC, Li B and Nie W. Arsenic trioxide inhibits cancer stem-like cells via down-regulation of Gli1 in lung cancer. Am J Transl Res 2016; 8: 1133-43.

[10] Bora-Singhal N, Perumal D, Nguyen J and Chellappan S. Gli1-mediated regulation of Sox2 facilitates self-renewal of stem-like cells and confers resistance to EGFR inhibitors in non-small cell lung cancer. Neoplasia 2015; 17: 538-51.

[11] Xie SY, Li G, Han C, Yu YY and Li N. RKIP reduction enhances radioresistance by activating the Shh signaling pathway in non-small-cell lung cancer. Onco Targets Ther 2017; 10: 5605-19.

[12] Ishikawa M, Sonobe M, Imamura N, Sowa T, Shikuma K and Date H. Expression of the GLI family genes is associated with tumor progression in advanced lung adenocarcinoma. World J Surg Oncol 2014; 12: 253.

[13] Armas-Lopez L, Pina-Sanchez P, Arrieta O, de Alba EG, Ortiz-Quintero B, Santillan-Doherty P, Christiani DC, Zuniga J and Avila-Moreno F. Epigenomic study identifies a novel mesenchyme homeobox2-GLI1 transcription axis involved in cancer drug resistance, overall survival and therapy prognosis in lung cancer patients. Oncotarget 2017; 8: 67056-81.

[14] Leprieur EG, Vieira T, Antoine M, Rozensztajn N, Rabbe N, Ruppert AM, Lavole A, Cadranel J and Wislez M. Sonic hedgehog pathway activation is associated with resistance to platinum-based chemotherapy in advanced non-small-cell lung carcinoma. Clin Lung Cancer 2016; 17: 301-8.

[15] Aoi T. Biology of lung cancer: genetic mutation, epithelial-mesenchymal transition, and cancer stem cells. Gen Thorac Cardiovasc Surg 2016; 64: 517-23.

[16] Miller TJ, McCoy MJ, Hemmings C, Bulsara MK, Iacopetta B and Platell CF. The prognostic value of cancer stem-like cell markers SOX2 and CD133 in stage III colon cancer is modified by expression of the immune-related markers FoxP3, PD-L1 and CD3. Pathology 2017; 49: 721-30.

[17] Zhang Y, Xu W, Guo H, Zhang Y, He Y, Lee SH, Song X, Li X, Guo Y, Zhao Y, Ding C, Ning F, Ma Y, Lei QY, Hu X, Li S and Guo W. NOTCH1 signaling regulates self-renewal and platinum chemoresistance of cancer stem-like cells in human non-small cell lung cancer. Cancer Res 2017; 77: 3082-91.

[18] Zhang M, Tan S, Yu D, Zhao Z, Zhang B, Zhang P, Lv C, Zhou Q and Cao Z. Triptonide inhibits lung cancer cell tumorigenicity by selectively attenuating the Shh-Gli1 signaling pathway. Toxicol Appl Pharmacol 2019; 365: 1-8.

[19] Jia H, Qi H, Gong Z, Yang S, Ren J, Liu Y, Li MY and Chen GG. The expression of FOXP3 and its role in human cancers. Biochim Biophys Acta Rev Cancer 2019; 1871: 170-8.

[20] Li H, Da LJ, Fan WD, Long XH and Zhang XQ. Transcription factor glioma-associated oncogene homolog 1 is required for transforming growth factor-beta 1-induced epithelial-mesenchymal transition of non-small cell lung cancer cells. Mol Med Rep 2015; 11: 3259-68.

[21] Qi HZ, Chen GS, Huang YX, Si ZZ and Li JQ. Foxp3-modified bone marrow mesenchymal stem cells promotes liver allograft tolerance through the generation of regulatory T cells in rats. J Transl Med 2015; 13: 274.

[22] Kasiri S, Shao C, Chen B, Wilson AN, Yenerall P, Timmons BC, Girard L, Tian H, Behrens C, Wistuba II, Gazdar AF and Kim J. GLI1 blockade potentiates the antitumor activity of PI3K antagonists in lung squamous cell carcinoma. Cancer Res 2017; 77: 4448-59.

[23] Yang S, Liu Y, Li MY, Ng CSH, Yang SL, Wang S, Zou C, Dong Y, Du J, Long X, Liu LZ, Wan IYP, Mok T, Underwood MJ and Chen GG. FOXP3 promotes tumor growth and metastasis by activating Wnt/beta-catenin signaling pathway and EMT in non-small cell lung cancer. Mol Cancer 2017; 16: 124.

[24] Shi L, Wang Y, Lu Z, Zhang H, Zhuang N, Wang B, Song Z, Chen G, Huang C, Xu D, Zhang Y, Zhang W and Gao Y. miR-127 promotes EMT and stem-like traits in lung cancer through a feed-forward regulatory loop. Oncogene 2017; 36: 1631-1643.

[25] Heng WS, Gosens R and Kruyt FAE. Lung cancer stem cells: origin, features, maintenance mechanisms and therapeutic targeting. Biochem Pharmacol 2019; 160: 121-33.

[26] Yue D, Li H, Che J, Zhang Y, Tseng HH, Jin JQ, Luh TM, Giroux-Leprieur E, Mo M, Zheng Q, Shi H, Zhang H, Hao X, Wang C, Jablons DM and He B. Hedgehog/Gli promotes epithelial-mesenchymal transition in lung squamous cell carcinomas. J Exp Clin Canc Res 2014; 33: 34.

[27] Santoni de Sio FR, Passerini L, Valente MM, Russo F, Naldini L, Roncarolo MG and Bacchetta R. Ectopic FOXP3 expression preserves primitive features of human hematopoietic stem cells while impairing functional T cell differentiation. Sci Rep 2017; 7: 15820.

[28] Udoh K, Parte S, Carter K, Mack A and Kakar SS. Targeting of lung cancer stem cell self-renewal pathway by a small molecule verrucarin J. Stem Cell Rev 2019; 15: 601-611.

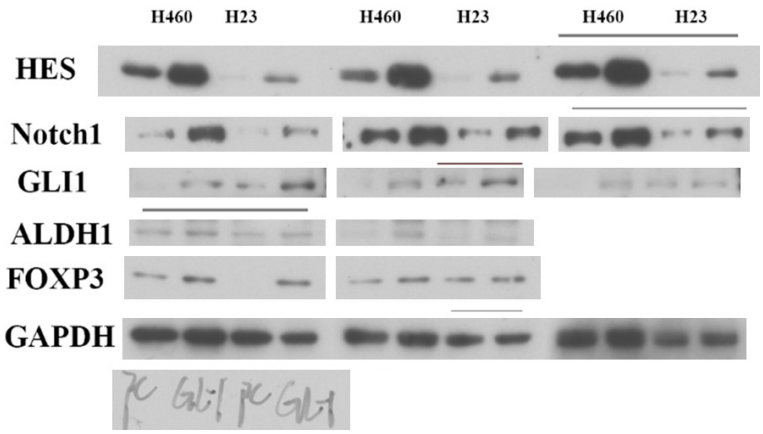

Supplementary Figure 1. Example of Western blot results.